Thermal signatures identify the influence of dams and ponds on stream temperature at the regional scale

Hanieh Seyedhashemi, Florentina Moatar, Jean-Philippe Vidal, Jacob Diamond, Aurélien Beaufort, André Chandesris, Laurent Valette

Thermal signatures identify the influence of dams and ponds on stream temperature at the regional scale

Hanieh Seyedhashemi[a,b*], Florentina Moatar[a], Jean-Philippe Vidal[a], Jacob S. Diamond[a,b], Aurélien Beaufort[a,b], André Chandesris[a], Laurent Valette[a]

[a]INRAE, UR RiverLy, centre de Lyon-Villeurbanne, 5 rue de la Doua CS 20244, 69625 Villeurbanne, France

[b]EA 6293 GéoHydrosystèmes COntinentaux, Université François-Rabelais de Tours, Parc de Grandmont, 37200 Tours, France

*Corresponding author: hanieh.seyedhashemi@inrae.fr

Florentina Moatar: florentina.moatar@inrae.fr

Jean-Philippe Vidal: jean-philippe.vidal@inrae.fr

Jacob S. Diamond: jacob.diamond@inrae.fr

Aurélien Beaufort: aurelien.beaufort@hotmail.fr

André Chandesris: andre.chandesris@inrae.fr

Laurent Valette: laurent.valette@inrae.fr

1 Abstract

Anthropogenic impoundments (e.g. large dams, small reservoirs, and ponds) are expanding in number globally, influencing downstream temperature regimes in a diversity of ways that depend on their structure and position along the river continuum. Because of the manifold downstream thermal responses, there has been a paucity of studies characterizing cumulative effect sizes at the catchment scale. Here, we introduce five thermal indicators based on the stream-air temperature relationship that together can identify the altered thermal signatures of dams and ponds. We used this thermal signature approach to evaluate a regional dataset of 330 daily stream temperature time series from stations throughout the Loire River basin, France, from 2008–2018. This basin (10^5 km^2) is one of the largest European catchments with contrasting natural and anthropogenic characteristics. The derived thermal signatures were cross-validated with several known catchment characteristics, which strongly supported separation into dam-like, pond-like and natural-like signatures. We characterize the thermal regime of each thermal signature and contextualize it using a set of ecologically relevant thermal metrics. Results indicate that large dams decreased summer stream temperature by 2°C and delayed the annual stream temperature peak by 23 days relative to the natural regimes. In contrast, the cumulative effects of upstream ponds increased summer stream temperature by 2.3°C and increased synchrony with air temperature regimes. These thermal signatures thus allow for identifying and quantifying downstream thermal and ecological influences of different types of anthropogenic infrastructures without prior information on the source of modification and upstream water temperature conditions.

Keywords: thermal regime, impoundment, reservoir, Loire River, thermal sensitivity

1. Introduction

1.1 Stream temperature in a changing world

River corridors store, transform, and convey mass and energy from headwaters to oceans. Although rivers are typically analyzed as lotic systems, the distribution of lentic water bodies (e.g., lakes, reservoirs, ponds) along the river continuum has recently come to light as a critical factor in nitrogen removal (Harrison et al., 2009; Schmadel et al., 2018), and storage of phosphorus (Grantz et al., 2014) and sediments (Vörösmarty et al., 2003). An emerging concern is the cumulative effects of lentic systems on stream and river water temperature, which is a critical parameter affecting the eutrophication of water bodies (Minaudo et al., 2018; Le Moal et al., 2019) and the distribution of aquatic communities (Cox & Rutherford, 2000; Poole & Berman, 2001; Ducharne, 2008).

Stream temperature effects from lentic water bodies depend strongly on their individual characteristics and their overall spatial distributions, complicating scales of inference and prediction. For example, anthropogenic features like dams, impoundments and ponds appear to have contrasting effects on stream temperature (Webb, 1996; Webb et al., 2008; Olden & Naiman, 2010). It is important to develop a more general understanding of these effects because global change will likely exacerbate them, e.g., by increasing the number of future dams or ponds and increasing the capacity of current ones. Indeed, in some countries, recurrent droughts led to an increase in the number of small farm dams storing water for later use in irrigation (Habets et al., 2013). The preponderance of studies on the regional scale effects of anthropogenic structures use physical process-based models that are highly parameterized (Van Vilet et al., 2012; Niemeyer et al., 2018; Yearsley et al., 2019; Cheng et al., 2020), limiting their broad applicability (Dugdale et al., 2017). Hence, there is a need for simpler, data-based tools that can identify and predict such anthropogenic effects on stream temperature and

subsequent consequences to ecosystems, particularly at large scales relevant to management.

1.2 Large dams tend to reduce stream temperature and shift annual cycles

The effects of large dams on river thermal regimes are well studied at the site scale (Webb & Walling, 1993, 1996, 1997; Lowney, 2000; Preece & Jones, 2002; Casado et al., 2013). These studies typically compare observed stream temperature regimes above and below the dam, before and after dam construction, or in regulated and unregulated streams, with unregulated streams being located in close proximity of regulated streams with a similar climate. Results provide strong support that large dams generally reduce downstream temperatures by releasing cold, hypolimnetic water in summer (Olden & Naiman, 2010), and that they delay the annual cycle of both flow (Lehner et al., 2011) and stream temperature regimes (Webb & Walling, 1993; Webb, 1996). Additionally, through discharge regime regulation (Petts & Gurnell, 2005), large dams may also modify stream temperature through the impact on thermal capacity without necessarily modifying the components of heat budget (Webb & Walling, 1996; Poole & Berman, 2001). While some subsequent works have used physical process-based models to upscale these effects across river networks and regions (Van Vliet et al., 2012; Niemeyer et al., 2018; Cheng et al., 2020; Daniels & Danner, 2020), large-scale empirical assessments remain scarce (but see Steel & Lange, 2007; Maheu et al., 2016a, Hill et al., 2013). Hence, there is still a major gap in our regional scale understanding of dam-induced alterations, largely because the changes to any one component of river thermal regime depend on the spatiotemporal scales considered (Steel & Lange, 2007).

1.3 Ponds and shallow reservoirs tend to increase stream temperature

Pond and shallow (<15 m in height) reservoir effects on stream temperature differ from those of large dams due to their mode of downstream water release. Observations

suggest that the surficial water release from these structures – as opposed to hypolimnetic release from large dams – tends to increase downstream stream temperature (Sinokrot et al., 1995; Maxted et al., 2005; Bae et al., 2016; Maheu et al., 2016b; Chandesris et al., 2019). The greatest increase in stream temperature occurs during low-flow periods (Webb, 1996). Specifically, these structures increase not just the average stream temperature, but also its diurnal range and the frequency and duration of high temperatures (Maheu et al., 2016a, 2016b; Chandesris et al., 2019). Further, the increase in downstream temperature is weakly compensated by natural processes, leading to minimal downstream recovery to baseline temperatures (Boon & Shires, 1976; Fraley, 1979; Maxted et al., 2005; Dripps & Granger, 2013). However, thermal alterations from small impoundments are far less studied than those of large dams, and their cumulative effects on river thermal regimes at the regional scale are unknown.

1.4 The stream-air temperature relationship as a diagnostic tool

A major challenge in the regional assessment of water temperature is the lack of detailed information about the heat budget (Webb & Zhang, 1997). This issue leads to using air temperature as a proxy for computing the river heat budget. Simple linear regression between water and air temperature is a common proxy technique to infer stream thermal regimes (Stefan & Preud'homme, 1993; Pilgrim et al., 1998; Mohseni et al., 1999; Erickson & Stefan, 2000; Caissie et al., 2004), but regression parameters are highly spatially variable. For instance, river reaches without groundwater input typically have steep regression slopes with low intercepts, but opposite relations can emerge for groundwater-dominated reaches (Caissie, 2006; O'Driscoll & DeWalle, 2006; Kelleher et al., 2012). The relationship between water temperature and air temperature may also be altered by different types of anthropogenic disturbances leading to a weaker correlation and/or a smaller regression slope (Erickson & Stefan, 2000; Webb et al., 2008; Bae et al.,

2016). We can therefore take advantage of these spatially variable relationships to infer the controls and drivers of stream temperature.

1.5 Thermal signatures as a means of identifying anthropogenic influences

We suggest development of "thermal signatures" based on air-water temperature relationships to identify anthropogenic influences on stream temperature regimes. The choice of the name thermal signatures derives from the analogous concept of hydrological signatures (Gupta et al., 2008), which use statistical analysis of flow regimes to provide information on broader controls on hydrological behavior (e.g., dominant flow processes, strength and spatiotemporal variability of the rainfall–runoff response (Berhanu et al., 2015; McMillan et al., 2017). Similarly, thermal signatures capitalize on indicators extracted from the statistical structure of local stream-air temperature relationships to identify the dominant processes (e.g., anthropogenic influences) that generate observed stream temperature time series. Due to the wide availability of air temperature data and the rapid growth of water temperature datasets, thermal signatures can be applied at large scales, facilitating regional assessments of stream temperature variability. Thermal signatures further allow tracing of systematic changes introduced by anthropogenic structures like dams or ponds, and identification of highly influenced reaches at large scale.

1.6 Purpose of the study

The purpose of this study is to distinguish the characteristics of altered and natural stream thermal regimes, and to determine their spatial distributions at a regional scale with a simple, data-based approach. To do so, we use novel thermal signatures based on both stream-air temperature linear regression and seasonality analysis. These signatures reveal the influence of dams and ponds on thermal regimes without prior information on the source of modification or upstream water temperature conditions. We then cross validate

our thermal signature approach with known properties of catchments and anthropogenic structures. Finally, we contextualize the thermal signatures with a set of ecologically relevant thermal metrics.

2 Study area and data

2.1 Loire basin and surface waters

The Loire basin is a large European catchment (10^5 km^2) with contrasting natural conditions (Figure 1), providing an ideal case study to test the limitations of the thermal signature approach. Mean annual precipitation (549–2130 mm), mean annual air temperature (6.0–12.5°C), altitude (10–1850 m), and lithology provide spatially variable controls on stream temperature regime (Figure 1, left panel.).

[Figure 1 about here.]

Surface waters (as identified by aerial photography; minimum resolution of 15 m^2) cover approximately 0.8% of the Loire basin, and include 11 natural lakes and numerous artificial ponds, shallow reservoirs (6 m< height <15 m), and large dams (height>15 m). Up to 70% of surface waters have surface areas less than 10 ha, and less than 0.5% of the surface waters (by number) are shallow reservoirs. Hence, over 99% of surface waters are artificial ponds, commonly dedicated to irrigation or recreation. Height and volume estimates are unavailable for the most of these artificial ponds (see Figure 1, right panel; IGN, 2006). Based on these observations, we considered surface waters that were not natural lakes or dams to be "ponds", while recognizing that some small proportion of these so-called ponds may indeed be shallow reservoirs.

The Loire River basin houses 73 large dams (total storage capacity, S=999 Mm^3), which are used for hydroelectricity (S=734 Mm^3), drinking water (S=57 Mm^3), recreation (S=32 Mm^3) and navigation (S=234 Mm^3) (see Figure 1, right panel). The two largest dams are: 1) Naussac dam (S=190 Mm^3, height =50 m), and 2) Villerest dam (S=106

166 Mm^3, height = 59 m) (Figure 1, right panel) These large dams are located in the upstream
167 part of the basin (referred to as region A in Figure 1, right panel), with granite and basalt
168 lithology and little influence of groundwater input.

169 *2.2 Observed stream and air temperature data*

170 We obtained hourly water temperature for 2008–2018 at 392 stations with complete
171 year data, most of which were managed by the French Agency for Biodiversity
172 (http://www.naiades.eaufrance.fr) and the National Fishing Federation
173 (https://www.federationpeche.fr). Most stations (55%) had at least 5 years of data, with
174 1% having all 11 years of complete temperature data and 33% having less than 3 years.
175 The stations are evenly distributed across the Loire basin, with a median Euclidean
176 distance between any two stations of 4 km. The stations represent a wide range of river
177 discharge (mean annual specific discharge 72–1050 mm y^{-1}) and width (1.5–34 m), with
178 75% of the stations located on rivers with a Strahler order from 2 to 4. The mean annual
179 stream temperature varies between 8°C in the upstream part of the basin and 14°C in the
180 western downstream part. The majority of stations (~80%) have artificial ponds in their
181 contributing area. There are 38 stations downstream of large dams (median of distance=6
182 km). For the large dams, no information about mode-of-operation (e.g., peaking, run-of-
183 river, storage, etc.) was available. Only four stations are located downstream of natural
184 lakes (median of distance=4.15 km).

185 We obtained air temperature data from SAFRAN reanalysis at a 8-km spatial
186 resolution (Quintana-Segui et al., 2008; Vidal et al., 2010). SAFRAN is a mesoscale
187 atmospheric analysis system for surface variables. It produces an analysis at the hourly
188 time step using ground data observations and numerical models. The daily-averaged data
189 of the closest grid cell to each stream temperature station is used.

2.3 Basin feature databases and descriptors

We used four databases to obtain catchment characteristics for each station:

- BD ALTI® 50-m resolution digital terrain model dataset for topographic variables (IGN, 2011);
- RHT (Theoretical Hydrographic Network for France, and its environmental attributes) for river and stream hydrological variables (Pella et al., 2012);
- BD CARTHAGE® (Thematic CARtography Database of Water Agencies and the Ministry of the Environment) for location and surface areas of reservoirs and ponds (IGN, 2006);
- AELB (Loire-Bretagne Water Agency) for dams' characteristics (location, height and volume) (Chandesris & Pella, 2006);
- SYRAH-CE (Relational System for Auditing River Hydromorphology) for land cover and geomorphological variables (Valette et al., 2012).

3 Methods

We define five general steps to identify and characterize thermal signatures of altered stream temperature regimes:

1. Select stream temperature stations;
2. define thermal indicators and signatures for identifying altered regimes;
3. identify thermal signatures of altered regimes through clustering based on thermal indicators;
4. cross validate the derived thermal signatures; and
5. characterize the thermal signatures.

3.1 Select stream temperature stations

We selected stations based on their potential to be influenced by anthropogenic structures. This effectively eliminates large rivers from our dataset because they are

weakly sensitive to thermal regime alterations due to their larger conveyed volumes and greater thermal capacity (Smith & Lavis, 1975; Webb & Walling, 1993; Caissie, 2006; Kelleher et al., 2012). Moreover, because large river temperatures are approximately in equilibrium with air temperature (Moatar & Gailhard, 2006; Bustillo et al., 2014), information extracted from regression-type analyses is equivocal. Therefore, this study focuses on smaller rivers to identify altered regimes.

To subset our original dataset to focus on smaller rivers, we removed stations that are in equilibrium with air temperature (and thus weakly sensitive to our proposed thermal signature approach) using a distance-from-source threshold. To calculate this threshold, we regressed interannual summer (June–August, referred to as "JJA" throughout) temperature means for both stream and air temperature against distance from headwater source (as derived from the RHT database), and extracted the intersection of the two regressions (Figure S1, left panel). Sites above the distance-from-source value at this intersection will be removed from further analysis.

3.2 Define thermal indicators and signatures for identifying altered regimes

Typically, upstream reference conditions are used to identify the downstream thermal alterations of anthropogenic structures. Since such information is in practice rather limited, air temperature may be used as a proxy for the heat budget reference conditions. As such, we propose five thermal indicators to identify the dominant process of thermal regime (Table 1 and Figure 2). The choice of these indicators is based on a preponderance of literature evidence on the known impacts of dams and ponds. In the following, T_w stands for stream (water) temperature and T_a for air temperature.

[Figure 2 about here.]

[Table 1 about here.]

The first two indicators are based on daily, summertime stream-air temperature linear

regressions. Stream-air temperature linear regression may be calculated on annual data (Kelleher et al., 2012; Beaufort et al., 2020) or summer data (Mayer, 2012). We selected the summer period to capture the higher influence of large dam operations on stream temperature during these months. The first derived thermal indicator is the regression slope between stream and air temperature, which we term "thermal sensitivity", or TS (°C °C^{-1}, or unitless [-]), because it indicates how sensitive stream temperature is to changes in air temperature (Kelleher et al., 2012). In natural streams, TS is greater when climate is the main control on stream temperature, but TS is lower where ground water inputs are large (Caissie, 2006; Mayer, 2012) or when dams reduce the temporal coupling between stream and air temperature. The second thermal indicator is the coefficient of determination (R^2) of the regression between stream and air temperature, which indicates the predictive capacity of air temperature on stream temperature, and therefore shows how strongly these variables are coupled (Kelleher et al., 2012). In natural streams, R^2 is high, whereas in streams with an upstream dam, R^2 is low, like TS.

The remaining three thermal indicators are derived from daily stream and air temperature time series. The first one is the "lag time" (days) between the annual peak of the two 30-days moving average time series. This indicator detects how dams delay the annual cycle (see Figure S2 for an example). The next indicator, which we term the "heating effect" (°C), is the mean positive difference of daily stream-air temperature (T_w-T_a) from March to October. This period is selected to avoid any snowmelt effect on stream temperature, and to have the greatest increase in stream temperature due to ponds during the low-flow period. This heating effect indicates how energy storage in ponds increases downstream stream temperature. The final indicator, which we term the "thermal effect" (°C), is the mean overall difference of daily stream-air temperature difference (T_w-T_a) from March to October. The thermal effect indicates overall temperature effects of ponds

on downstream waters, accounting for potential natural cooling and mitigation of heating effects. We calculated the five indicators at each station for each year with data and computed their interannual means for further analysis.

We hypothesized that because TS, R^2, and lag time are able to capture the impacts of managed dams—indeed, dams decrease TS and R^2 (Webb et al., 2008, and see Figure S3), and delay the annual cycle (Webb & Walling, 1993; Webb, 1996)—they would reveal a *dam signature* on thermal regimes (Table 1). Similarly, we hypothesized that the remaining two indicators–the heating effect and the thermal effect–would detect the influence of energy storage observed in the presence of artificial ponds (Dripps & Granger 2013, Chandesris et al. 2019, and see Figure S2), and thus reveal a *pond signature* on thermal regimes (Table 1).

3.3 Identify thermal signatures of altered regimes through clustering based on thermal indicators

The objective of this step is to cluster stations using the scaled values of five thermal indicators defined in Table 1. We used K-means clustering (with Euclidean distance), which is an unsupervised learning algorithm that partitions n observations into k clusters, where each observation belongs to the cluster with the nearest mean. An optimal number of clusters was obtained using the *NbClust* R package (Charrad et al., 2014; R Core Team, 2013). This package provides 30 popular indices that determine the number of clusters in a data set by using k-means clustering method, and offers the user the best clustering scheme based on different results. The number of clusters suggested by the majority of these indices was selected.

3.4 Cross validate derived thermal signatures

We validated the derived thermal signature clusters in three ways, each based on the expectation that stations clustered together would have similar catchment properties and

anthropogenic features. In the first step, we used a simple presence/absence test for upstream human-constructions (i.e., does the station have an upstream pond or dam?). We then calculated odds-ratios for each cluster from presence/absence counts of upstream dams or ponds to determine the strength of association between clustering based on thermal indicators and known anthropogenic influence. For example, for a cluster with a dam thermal signature, we calculated the ratio between the odds of being in that cluster given presence of a dam and the odds of being in the cluster given the absence of a dam.

Second, to test how well the clusters aligned with specific anthropogenic features, we compared statistical distributions of dam and pond characteristics (Table 2) among the clusters using ANOVA and the post-hoc Tukey's Honestly Significant Difference t-test with Bonferroni adjustment. Prior to any analyses, we ensured homogeneity of variances and normality using log transformation when necessary. Because the cross validation data relies on measured dam and pond characteristics, these analyses were conducted on subsets of stations with known dams (n=38) and ponds (n=260). We hypothesized that stations from respective dam- or pond-like clusters would have greater or lower values of their respective feature characteristics. For example, we expected that stations from the dam cluster would have a much smaller distribution of distance to the closest dam than the other clusters, or that stations from the pond cluster would have a higher proportion ponded surface area than the other clusters. Hence, this provides a more detailed validation than the simple presence/absence test.

Finally, we validated the dam/pond thermal signature clustering using catchment-specific dam and pond characteristics in the presence of other natural landscape predictors as controlling factors. To do so, we used stepwise linear regression (*MASS* package in R; Venables & Ripley, 2002) to select the catchment, dam, or pond characteristics (Table 2) that best explained their respective thermal indicators. We chose our catchment

315 descriptive variables based on hypothesized controls on thermal regimes, and a
316 preliminary multi-collinearity assessment using various diagnostic tests from the *mctest* R
317 package (Imdadullah et al., 2016).

318 [Table 2 about here.]

319 *3.5 Characterize the thermal signatures*

320 We first characterized the derived thermal signatures by comparing their aggregate
321 stream and air temporal behaviors. The goal was to create a portrait of how the respective
322 cumulative effects of dams and ponds modulated stream temperature relative to air
323 temperature and relative to so-called "natural" regimes. We also sought to place the
324 altered thermal regimes in the context of widely used ecological metrics. To do so, we
325 gathered metrics from biodiversity and stream ecology (Verneaux et al., 1977; Buisson &
326 Grenouillet, 2009; Steel et al., 2017; Table 3) to quantitatively evaluate anthropogenic
327 effects in altered regimes compared to natural ones. We then compared the means of these
328 thermal metrics from altered regimes to those from natural regimes using ANOVA and
329 the post-hoc Tukey's Honestly Significant Difference t-test with Bonferroni adjustment
330 (natural regimes was used as the reference group). We excluded false-positives (e.g.,
331 stations that were clustered in a dam thermal signature, but did not have a dam) from this
332 analysis to avoid misinterpretation of true anthropogenic effects.

333 [Table 3 about here.]

334 4 **Results**

335 *4.1 Selected stations*

336 Our distance-from-source analysis found that 100 km approximately delineated the
337 designation between small and large rivers (Figure S1). Large rivers in this sense were
338 rivers with stream temperature in equilibrium with air temperature and less sensitive to the
339 human induced alterations (Figure S1, right panel). These stations are therefore excluded,

340 resulting in 330 stations with a median catchment area of 232 km^2 (range=3–1600 km^2).

341 *4.2 Thermal indicator distributions*

342 [Figure 3 about here.]

343 Thermal indicator distributions tended to group together based on their hypothesized
344 thermal signature (i.e., dam or pond; Figure 3). TS was spatially variable across the region
345 and lacked clear patterning, although most low TS (i.e., TS<0.2) stations were located in
346 the upstream part of basin (Figure 3). In contrast, the spatial distributions of R^2 and lag
347 time varied much less, covaried with each other, and were more spatially homogeneous.
348 Indeed, 83% of stations had both high R^2 (i.e., >0.6), and short lag times (i.e., <20 days).
349 Visual inspection revealed that stations with low TS coincided with lower values of R^2
350 (<0.6), and higher values of lag time (>30 days) in the upstream part of the basin. Ranges
351 for heating and thermal effects were 0.05°C to 4°C and −4.9°C to 3.7°C, respectively, but
352 the interquartile ranges were much narrower: 0.54°C to 1.14°C and -1.58 to 0.16,
353 respectively. Stations with larger heating effects (e.g., >1°C), tended to exhibit greater
354 thermal effects (e.g., >1°C) as well (r=0.9).

355 *4.3 Clustering the stations into thermal signatures*

356 The greatest proportion of indices (11 out of 30) suggested an optimal number of three
357 clusters based on the five thermal indicators. The stations in cluster 1 are located in the
358 upstream part of the basin (zone A of Figure 1). The stations in cluster 2 are scattered over
359 the basin, and 60% of the stations in cluster 3 tend to be found in the upstream part of the
360 basin (see the bottom right panel of Figure 3).

361 [Figure 4 about here.]

362 The statistical distribution of thermal indicators within each cluster suggests the proper
363 labelling of the obtained clusters with regard to the underlying physical processes (Figure
364 4). First, the lowest median values of TS (0.22) and R^2 (0.23) are observed in cluster 1,

along with the greatest median value of lag time (26 days). Therefore, we label cluster 1 as dam-like. Second, the greatest median values of TS (0.42), heating effect (1.38°C), and thermal effect (0.65°C) are found in cluster 2. The second cluster is thus labelled as pond-like. Finally, the median value of TS in stations that belong to cluster 3 (0.34) is closer to the median value of TS in the stations in the pond-like cluster than that of the stations in the dam-like cluster. Stations in cluster 3 also exhibit the highest median value of R^2, and the smallest heating or thermal effects. In this regard, cluster 3 is labelled as natural-like.

4.4 Cross validation of derived clusters

4.4.1 Presence-absence test

The plausibility of the clustering results was validated by the presence/absence test of dams and ponds in each cluster. In support of our labelling scheme, 71% of stations in the dam-like cluster had an upstream dam and if a site contained an upstream dam, it was 31.1 times more likely ($p < 0.001$) to be in the dam-like cluster than if it did not have an upstream dam. Similarly, 94% of stations in the pond-like cluster have ponds in their catchment and if a site contained an upstream pond, it was 6.5 times more likely ($p < 0.001$) to be in the pond-like cluster than if it did not have an upstream pond. The lower odds-ratio for the pond-like cluster is due to the high proportion of stations (49% of all stations) outside of this cluster that did have upstream ponds (i.e., were false negatives). Indeed, 72% of stations in the natural-like cluster have ponds in their catchment.

4.4.2 Dam and pond characteristic distributions

The statistical distribution of dam descriptive variables differed from each other among the clusters—IRI ($F_{1,30}$=7.307, p=0.01), d_{dam} ($F_{1,34}$=9.120, p=0.005), and IRI/d_{dam} ($F_{1,30}$=4.84, p=0.035)—and clearly supported the clustering results (Figure S4). Dam-like stations were located closer to their upstream dam (median=4.5 km) compared to the pond-like stations (median=10 km; t_{19}=-4.078, p=0.001) and natural-like stations

(median=6.5 km; t_{15}=-2.769, p=0.014). Similarly, dam-like stations had upstream dams that were an order of magnitude larger (implied by larger values of IRI, median=14.3%) than dams upstream of pond-like stations (median=0.36%; t_{14}=3.555, p=0.003) and natural-like stations (median=3.7%; t_{17}=2.809, p=0.012).

The mean values of pond descriptive variables also differed from each other among the clusters, but the differences were less clear than for dam descriptive variables—$f_{pond,reach}$ ($F_{2,205}$=0.031, p=0.97), $\bar{f}_{pond,reach}$ ($F_{2,205}$=0.016, p=0.854), and $f_{pond,catchment}$ ($F_{2,257}$=5.967, p=0.003) (Figure S5). Although statistically insignificant, pond-like stations had over twice as much ponded reach area than natural like stations at both the local reach scale (median $f_{pond,reach}$=6.5% versus 3.0%; t_{157}=0.235, p=0.815) and the catchment scale (median $\bar{f}_{pond,reach}$=1.4% versus 0.6%; t_{179}=0.557, p=0.578). These results were mirrored by overall proportional ponded area at the catchment scale (i.e., not just along reaches) for pond-like and natural-like stations (median $f_{pond,catchment}$=0.14% versus 0.07%; t_{173}=3.702, p=0.001). The dam-like cluster was not analyzed with t-tests because we reasoned that the stream temperature regime resets at the dam position and the cumulative effects of ponds will be lost.

4.4.3 Multiple regression with catchment variables

[Table 4 about here.]

The stepwise multiple regression procedure broadly supported the clustering results, and indicated that dam and pond characteristics are the strongest controls on thermal indicators and therefore on thermal signatures. Indeed, of the 10 considered catchment variables, only two arose as being important predictors of or controlling factors on thermal indicators (Table 4). For thermal indicators of the dam signature, only lag time was influenced by catchment slope, and for the pond signature, the heating effect was influenced by vegetation. More important were dam

characteristics: the closer a station is to a dam (low d_{dam}), and the bigger the dam (high IRI) the lower the TS and R^2; lag time also increased at stations that were closer to a dam. The influence of d_{dam} on TS was approximately 50% stronger than IRI, but d_{dam} influence on R^2 was approximately 20% weaker than IRI (based on scaled regression coefficients, Table 4). For lag time indicator, the influence of d_{dam} was 13% stronger than catchment slope. For ponds, ponded catchment area ($f_{pond,catchment}$) was the most important predictor variable of both heating and thermal effects, but percentage vegetation cover (Veg%) appeared to partially mitigate heating effects (at approximately half the influence of $f_{pond,catchment}$).

4.5 Characterize the thermal signatures

[Figure 5 about here.]

Thermal portraits from the three clusters supported current understanding on how anthropogenic structures influence stream and river thermal regimes (Figure 5). Compared to natural regimes, temperatures of dam-like stations exhibited downshifted (by 2°C) and lagged summer thermal peaks (by 23 days), with less clear differences in winter. In contrast, stream temperature of pond-like stations remains above air temperature over the whole year and is nearly synchronous with air temperature, mimicking the regimes of large rivers (Figure S1). Indeed, annual stream temperature amplitude of pond-like stations was 14°C, 15% less than that of large rivers (16.5°C), but 30–55% greater than that of dam-like or natural stations. Natural-like stations stand out in that their summer peaks are cooler than pond-like stations, but are warmer and more synchronous with air temperature than dam-like stations.

[Figure 6 about here.]

Altered thermal regimes (i.e., dam- and pond-like) clearly separated from natural regimes along ecological metrics— $\overline{T}_{w,summer}$ (F_{322}=17.625, p<0.001), max($T_{w,month}$)

(F_{322}=20.719, p<0.001), $N_{Tw>20}$ (F_{322}=55.529, p<0.001), $D_{Tw>15}$ (F_{320} =38.928, p<0.001), and max(ΔT_w) (F_{322}=39.786, p<0.001). Magnitude and frequency ($\overline{T}_{w,summer}$ and $N_{Tw>20}$) thermal metrics were less for dam-like stations than for natural-like stations (by 2°C, t_{15}=3.633, p=0.02; and 4 days, t_{32}=4.204, p=0.001), but frequency, duration, and rate of change thresholds were equivocal (Figure 6).

Altered thermal regimes from ponds differed from natural regimes along every thermal metric considered here, with a 2.3°C increase in average $\overline{T}_{w,summer}$ (t_{182}=-11.603 , p<0.001), a 2.5°C increase in max($T_{w,month}$) (t_{169}=-9.3, p<0.001), a 15-day increase in $N_{Tw>20}$ (t_{104}=-9.504, p<0.001), a 39-day increase in $D_{Tw>15}$ (t_{150}=-10.119, p<0.001), and a 2.6°C increase in ΔT_w (t_{210}=-12.345, p<0.001).

5 **Discussion**

Our results demonstrate that five simple indicators derived from stream-air temperature time series are capable of identifying the extent and characteristics of both altered and natural stream thermal regimes. Using these indicators, we could accurately parse the divergent thermal signatures of dams and ponds on the thermal regimes of flowing waters.

5.1 Large dam thermal signature

The spatial clustering of dam thermal signatures into the upstream of the Loire River basin aligned with the known distribution of dams there (Figure 1). This thermal signature approach may therefore be useful in identifying areas with strong thermal alteration from dam proliferation, like in the Amazon headwaters (Anderson et al. 2018).

Dam mode of operation affects its degree of change in downstream thermal regime (Olden & Naiman, 2010; Maheu et al., 2016a) and should be reflected in its emergent thermal signature. Our observed dam thermal signature was based on hypothesized cooling effects from hypolimnetic release, and although most stations downstream of

large dams exhibited this signature, many did not, suggesting alternative modes of operation. Hence, in future works, subsequent use of alternative thermal indicators to capture other modes of operation may be warranted. Even dams with the same purpose could have different mode of operation (Maheu et al., 2016a). Interannual variability driven by climate, adding an additional layer of complexity that may be difficult to assess with this method. Regardless, even the relatively simple approach here was largely successful in identifying altered thermal regimes. We provide additional evidence here that dams which release hypolimnetic water disrupt the stream-air temperature relationship (R^2) (Buendía et al. 2015), and delay the annual stream temperature peak (Olden & Naiman, 2010) (Figures 4 and 5).

The degree of dam thermal alterations depends on reservoir volume, stream order, and distance from the dam (Webb et al., 2008; Batalla et al., 2004). Here, we also show that channel slope is an important compounding factor on dam influence, which appeared to amplify lag time effects from dam proximity (Table 4): the steeper the channel, the less travel time there is for water-air equilibrium and thermal lag time increases. Our cross validation results also highlight the critical effect of dam volume on thermal regimes, underscoring previous works that identified a critical impoundment threshold of 5–20% of the mean annual runoff (Buendía et al. 2015; Maheu et al. 2016a). Importantly, we found that IRI>20% completely erased stream-air temperature correlation (data not shown; cf. Buendía et al. 2015). Stations with the weakest dam signature were far from large dams, supporting the known reduction of dams influence on thermal regimes (increase of TS) with distance due to the heat exchange with ambient conditions (Preece & Jones, 2002; Buendía et al., 2015). The coupling of greater distance from dam and lower IRI of upstream dam may provide additional explanation as to why 17 stations with known dams did not cluster into our dam-like thermal signature.

The induced changes by dams in ecologically relevant thermal metrics on downstream temperature were moderate. We observed effects of decreased summer stream temperatures and a large decrease in the frequency of high temperatures, in accordance with previous works (Olden & Naiman, 2010; Maheu et al., 2016a), but found little evidence for other ecologically relevant effects compared to natural systems. However, our focus was biased towards increased thermal alterations, and further metrics and analysis would benefit future inference.

5.2 Pond thermal signature

Ponds and shallow (<15 m in height) reservoirs impound water for different purposes that depend on location and local needs. We observed that ponds were evenly distributed throughout the Loire basin, with no clear clustering of sizes (Figure 1, right panel). In support of this observation, pond-like thermal signatures were evident throughout the basin (Figure 3), located mostly on medium size streams (median of distance from source=40 km).

Ponds typically release warm water from overflow, increasing downstream temperatures synchrony with air temperature (Dripps & Granger 2013, Maheu et al., 2016b). The pond thermal signature identified here aligns with other empirical results (Chandesris et al., 2019) and this general conceptual model (Figures 4 and 5). Stations influenced by small dams experience a small decrease in R^2, compared to natural stations (cf. Bae et al., 2016), which we also observed to a small degree (Figure 4). The extent of the induced change by ponds depends mostly on the surface area and residence time (Maxted et al., 2005; Chandesris et al., 2019). The lack of data on the depth of the pond/shallow reservoirs at this scale prevented us from using residence time. A bigger surface area, or a bigger residence time increase the time of exposure to air temperature and incoming solar radiation, leading to greater sensitivity of stream temperature to air

temperature (increased TS) (Maheu et al., 2016b; Michel et al., 2020). We also detected greater TS (thermal sensitivity) for pond-like stations (see Figure 4).

The single best predictor of the pond thermal signature was the proportion of a station's catchment that was ponded, strongly implying that pond effects have an emergent, cumulative effect on stream temperature regimes. Indeed, of the local, reach-scale metrics, neither could differentiate the thermal indicators or signatures (Table 4, Figure S5). However, we note that the reach scale metrics were defined based on recorded surface waters in 2011 and are perhaps not temporally aligned with stream and air temperature measurements used here. Importantly, our cross validation suggests that the thermal influence of ponds may be mitigated by vegetation cover (Maxted et al., 2005), suggesting the strategic planting of canopy cover species in thermal restoration efforts.

Ponds can alter ecologically relevant thermal metrics substantially. They increase the summer temperatures, frequency and duration of high temperatures (Lessard & Hayes, 2003; Maheu et al., 2016a, 2016b; Chandesris et al. 2019) which we found as well (see Figure 6).

5.3 Natural regimes

The thermal regimes of natural-like stations are those that are most strongly driven by natural factors like climate, topography, vegetative shading, and stream discharge (Poole & Berman, 2001; Kelleher et al., 2012; Hannah & Garner, 2015). These thermal signatures should therefore arise in regions with minimal anthropogenic influence, which we observed in their spatial clustering predominately in the upstream part of the Loire River basin where there is the greatest proportion of vegetation cover (cf. Beaufort et al., 2020). These natural stations were located on smaller streams (median of distance from source=24 km) and had typically greater proportions of vegetative cover (median of vegetation cover within a 10 meter buffer=100%).

Natural-like thermal signatures, unlike altered ones, had strong correlation with air temperature (cf. Webb et al., 2008) and exhibited minimal lag time, heating, or thermal effects (Figure 4). In accordance with Beaufort et al. (2020), who studied the controlling factors of natural regimes the Loire River basin, TS at the stations located on large rivers where climate is the key driver of stream temperature (median=0.43), was greater than the TS in natural-like stations (median=0.34). However, the values of TS in our study were smaller than the TS values reported by Beaufort et al. (2020), since the present study has focused on summer TS values. A similar result (median of TS=0.45) was obtained in an analysis focused on August stream temperatures, that attributed decreased summer TS to ground water input (Mayer 2012). In the current study, TS in the stations located in region B (Figure 1), which has the greatest potential for ground water input, was lower than TS in the stations located in regions A, and C (median TS=0.29 versus 0.35). Supporting our thermal signature approach, we observed annual amplitude for stations with natural thermal signatures (median=11°C) in direct accordance of observations in Beaufort et al., (2020) (9–14°C).

5.4 Limitations of the study

The stream temperature database used in the current study only includes stations with complete annual data, but less complete databases may struggle with the outlined approach. For example, when we also included 170 stations that only had summer data in our analysis, we observed that the lag time indicator was highly sensitive to within-year data availability, indicating that a year-round dataset is required for clustering. However, the pond signature indicators (heating and thermal effects) were not sensitive to within-year data availability, even when the summer stream temperature data were available. Importantly, if complete annual data are not available, the indicators appear quite robust to interannual data heterogeneity (i.e., missing whole years of data; Figure S6). The only

565 exception is lag time indicator, which can be heavily influenced by year-to-year variations
566 in both climate and upstream reservoir management.

567 The large sample size used in the present study, the presence of different types of
568 reservoirs over the study area, and the blind-eye towards dam operation may have some
569 implications for generalizing our findings. For example, in regions with more variable
570 dam operations, different clusters may arise, or it may be difficult to perform cluster
571 analysis without additional thermal indicators. Scales of inference are also likely to vary
572 among regions. In our study, we had a low possibility of station pseudo-replication due to
573 high resolution of SAFRAN data (8 km): only 20% of the SAFRAN meshes included
574 more than one station, and only 12% of the meshes included the stations with the same
575 clustering group. Hence, it is imperative to verify and cross-validate this approach when
576 applied to new datasets.

577 *5.5 Implications and perspectives*

578 The proposed thermal signatures approach allows a simple, rapid, and accurate
579 workflow to identify river reaches that are highly influenced by dams and ponds. The
580 methodology is inherently regional, aligning in scale with the jurisdictions of most
581 environmental agencies and working groups. We suggest that thermal signature results
582 can be used to identify hotspots and target specific reaches for restoration and further
583 investigation, and to more broadly design strategic measurement networks (Jackson et al.,
584 2016). Thermal signatures can also identify natural reaches as benchmarks for restoration
585 or aquatic species habitat protection. Indeed, there is much interest in predicting the
586 phenological and spatial diversity within species of interest or their prey (Steel et al.,
587 2017). Moreover, because climate change will likely exacerbate the degree of thermal
588 alterations (Michel et al., 2020) through increasing air temperature, decreasing
589 streamflow, and increasing demand for ponds and dams (Webb, 1996; Moatar & Gailhard,

2006), the thermal signature framework could be used to plan pond and dam placement to minimize cumulative downstream effects.

The proposed thermal signatures may also be used by modelers to develop a reference-condition model by the use of natural regimes (Hill et al., 2013), or to assess the performance of distributed water temperature models that do not take into account anthropogenic activities. The differences between simulated and observed thermal signatures at altered stations can serve as a bias correction factor that is a function of known dam or pond descriptive variables.

The thermal signature approach is flexible and can easily be reimagined for the other purposes other than detection and characterization of altered regimes from anthropogenic impoundments. For example, the stream-air temperature linear regression calculated on annual data could identify varied thermal signatures of ground water inputs in natural streams (with a focus on TS and the intercept) (Kelleher et al., 2012; Beaufort et al., 2020). Moreover, the synthesis of thermal signatures and hydrological signatures could be applicable in analyzing fish and macroinvertebrate communities.

6 Conclusions

Thermal signatures enable rapid and clear evaluation of the cumulative impact of human impoundments on stream temperature, highlighting two dominant modes of thermal alteration in the Loire River basin. We expect that the application of the thermal signatures will reveal new, possibly overlooked, modes of alteration depending on where it is applied, resulting in new perspectives on the growing spatiotemporal effects of anthropogenic structures to thermal regimes. Ultimately, by identifying natural thermal regimes, thermal signatures provide important information to managers on reference conditions, and can be used in conjunction with distributed models to identify bias, leading to improved performance and predictive capacity.

7 Acknowledgements

This work was realized in the course of a doctoral project at University of Tours, funded by European Regional Development Fund (Fonds Européen de développement Régional-FEDER) POI FEDER Loire no2017- EX001784, and Le plan Loire grandeur nature, Agence de l'eau Loire-Bretagne (AELB). The SAFRAN database was provided by the French national meteorological service (Météo-France). Stream temperature data were provided by the Office français de la biodiversité (OFB) and Fédération de Pêche (fishing federation).

8 References

Anderson, E. P., Jenkins, C. N., Heilpern, S., Maldonado-Ocampo, J. A., Carvajal-Vallejos, F. M., Encalada, A. C., ... & Salcedo, N. (2018). Fragmentation of Andes-to-Amazon connectivity by hydropower dams. Science Advances, 4(1), eaao1642.

Bae, M. J., Merciai, R., Benejam, L., Sabater, S., & García-Berthou, E. (2016). Small weirs, big effects: disruption of water temperature regimes with hydrological alteration in a Mediterranean stream. River Research and Applications, 32(3), 309-319. doi: https://doi.org/10.1002/rra.2871.

Batalla, R. J., Gomez, C. M., & Kondolf, G. M. (2004). Reservoir-induced hydrological changes in the Ebro River basin (NE Spain). Journal of Hydrology, 290(1-2), 117-136. doi: https://doi.org/10.1016/j.jhydrol.2003.12.002.

Beaufort, A., Moatar, F., Sauquet, E., Loicq, P., & Hannah, D. M. (2020). Influence of landscape and hydrological factors on stream–air temperature relationships at regional scale. Hydrological Processes, 34(3), 583-597. doi: https://doi.org/10.1002/hyp.13608.

Berhanu, B., Seleshi, Y., Demisse, S. S., & Melesse, A. M. (2015). Flow regime classification and hydrological characterization: a case study of Ethiopian rivers. Water, 7(6), 3149-3165. doi: https://doi.org/10.3390/w7063149.

Boon, P. J., & Shires, S. W. (1976). Temperature studies on a river system in north-east

642 England. Freshwater Biology, 6(1), 23-32. doi: https://doi.org/10.1111/j.1365-
643 2427.1976.tb01587.x.
644 Buendía, C., Sabater, S., Palau, A., Batalla, R. J., & Marcé, R. (2015). Using equilibrium
645 temperature to assess thermal disturbances in rivers. Hydrological Processes,
646 29(19), 4350-4360. doi: https://onlinelibrary.wiley.com/
647 doi/epdf/10.1002/hyp.10489.
648 Buisson, L., & Grenouillet, G. (2009). Contrasted impacts of climate change on stream
649 fish assemblages along an environmental gradient. Diversity and Distributions,
650 15(4), 613-626. doi: https://doi.org/10.1111/j.1472-4642. 2009.00565.x.
651 Bustillo, V., Moatar, F., Ducharne, A., Thiéry, D., & Poirel, A. (2014). A multimodel
652 comparison for assessing water temperatures under changing climate conditions via
653 the equilibrium temperature concept: case study of the Middle Loire River, France.
654 Hydrological Processes, 28(3), 1507-1524..doi: https://doi.org/10.1002/hyp.9683.
655 Caissie, D., St-Hilaire, A., & El-Jabi, N. (2004, June). Prediction of water temperatures
656 using regression and stochastic models. In 57th Canadian Water Resources
657 Association Annual Congress., Montreal (Vol. 6).
658 Caissie, D. (2006). The thermal regime of rivers: a review. Freshwater biology, 51(8),
659 1389-1406. doi: https://doi.org/10.1111/j.1472-4642.2009.00565.x.
660 Casado, A., Hannah, D. M., Peiry, J. L., & Campo, A. M. (2013). Influence of dam-
661 induced hydrological regulation on summer water temperature: Sauce Grande
662 River, Argentina. Ecohydrology, 6(4), 523-535. doi: https://doi.org/
663 10.1002/eco.1375.
664 Chandesris, A., & Pella, H. (2006). Constitution d'une base d'information spatialisée
665 «barrages, retenues et plans d'eau» au niveau national en vue d'évaluer les
666 modifications hydro-morphologiques (Doctoral dissertation, irstea). URL:
667 https://hal.inrae.fr/hal-02587668.
668 Chandesris, A., Van Looy, K., Diamond, J. S., & Souchon, Y. (2019). Small dams alter
669 thermal regimes of downstream water. Hydrology and Earth System Sciences, 23,

4509-4525. doi: https://doi.org/10.5194/hess-23-4509-2019.

Charrad, M., Ghazzali, N., Boiteau, V., Niknafs, A., & Charrad, M. M. (2014). Package 'nbclust'. Journal of statistical software, 61, 1-36. doi: http://dx.doi.org/10.18637/jss.v061.i06

Cheng, Y., Voisin, N., Yearsley, J. R., & Nijssen, B. (2020). Reservoirs modify river thermal regime sensitivity to climate change: a case study in the southeastern United States. Water Resources Research, 56(6), e2019WR025784. doi: https://doi.org/10.1029/2019WR025784.

Cox, T. J., & Rutherford, J. C. (2000). Predicting the effects of time-varying temperatures on stream invertebrate mortality. New Zealand Journal of Marine and Freshwater Research, 34(2), 209-215. doi: https://doi.org/10. 1080/00288330.2000.9516927.

Daniels, M. E., & Danner, E. M. (2020). The Drivers of River Temperatures Below a Large Dam. Water Resources Research, 56(5), e2019WR026751. doi: https://doi.org/10.1029/2019WR026751.

Dripps, W., & Granger, S. R. (2013). The impact of artificially impounded, residential headwater lakes on downstream water temperature. Environmental Earth Sciences, 68(8), 2399-2407. doi: https://doi.org/10.1007/ s12665-012-1924-4.

Ducharne, A. (2008). Importance of stream temperature to climate change impact on water quality. URL: https://hal.archives-ouvertes.fr/hal-00330876.

Dugdale, S. J., Hannah, D. M., & Malcolm, I. A. (2017). River temperature modelling: A review of process-based approaches and future directions. Earth-Science Reviews, 175, 97-113. doi: https://doi.org/10.1016/j.earscirev.2017.10.009.

Erickson, T. R., & Stefan, H. G. (2000). Linear air/water temperature correlations for streams during open water periods. Journal of Hydrologic Engineering, 5(3), 317-321. doi: https://doi.org/10.1061/(ASCE)1084-0699(2000) 5:3(317).

Fraley, J. J. (1979). Effects of elevated stream temperatures below a shallow reservoir on a cold water macroinvertebrate fauna. In The ecology of regulated streams (pp.

257-272). Springer, Boston, MA. doi: https://doi.org/10.1007/978-1-4684-8613-1_15.

Grantz, E. M., Haggard, B. E., & Scott, J. T. (2014). Stoichiometric imbalance in rates of nitrogen and phosphorus retention, storage, and recycling can perpetuate nitrogen deficiency in highly-productive reservoirs. Limnology and Oceanography, 59(6), 2203-2216. doi: https://doi.org/10.4319/lo.2014.59.6.2203.

Gupta, H. V., Wagener, T., & Liu, Y. (2008). Reconciling theory with observations: elements of a diagnostic approach to model evaluation. Hydrological Processes: An International Journal, 22(18), 3802-3813. doi: https://doi.org/10.1002/hyp.6989.

Habets, F., Boé, J., Déqué, M., Ducharne, A., Gascoin, S., Hachour, A., Martin, E., Pagé, C., Sauquet, E., Terray, L. and Thiéry, D. (2013). Impact of climate change on the hydrogeology of two basins in northern france. *Climatic change*, *121* , 771–785. doi: https://doi.org/10.1007/s10584-013-0934-x.

Hannah, D. M., & Garner, G. (2015). River water temperature in the United Kingdom: changes over the 20th century and possible changes over the 21st century. Progress in Physical Geography, 39(1), 68-92. doi: https://doi.org/10.1177/2F0309133314550669.

Harrison, J. A., Maranger, R. J., Alexander, R. B., Giblin, A. E., Jacinthe, P. A., Mayorga, E., ... & Wollheim, W. M. (2009). The regional and global significance of nitrogen removal in lakes and reservoirs. Biogeochemistry, 93(1-2), 143-157. doi: https://doi.org/10.1007/s10533-008-9272-x.

Hill, R. A., Hawkins, C. P., & Carlisle, D. M. (2013). Predicting thermal reference conditions for USA streams and rivers. Freshwater Science, 32(1), 39-55. doi: https://doi.org/10.1899/12-009.1.

IGN (2006). Descriptif technique bd carthage. URL: https://geoservices.ign.fr/ressources_documentaires/Espace_documentaire/BASES_VECTORIELLES/BDCARTHAGE/DL_BDCARTHAGE_3_0.pdf

IGN (2011). Descriptif technique bd alti, URL: https://geoservices.ign.fr/ressources_documentaires/Espace_documentaire/MODELES_3D/BDALTIV2/DC_BDALTI_2-0.pdf

Imdadullah, M., Aslam, M., & Altaf, S. (2016). mctest: An R Package for Detection of Collinearity among Regressors. R J., 8(2), 495.

Jackson, F. L., Malcolm, I. A., & Hannah, D. M. (2016). A novel approach for designing large-scale river temperature monitoring networks. Hydrology Research, 47(3), 569-590. doi: https://doi.org/10.2166/nh.2015.106.

Kelleher, C., Wagener, T., Gooseff, M., McGlynn, B., McGuire, K., & Marshall, L. (2012). Investigating controls on the thermal sensitivity of Pennsylvania streams. Hydrological Processes, 26(5), 771-785. doi: https://doi.org/10.1002/hyp.8186.

Lamouroux, N., Pella, H., Vanderbecq, A., Sauquet, E., & Lejot, J. (2010). Estimkart 2.0: Une plate-forme de modèles écohydrologiques pour contribuer à la gestion des cours d'eau à l'échelle des bassins français. Version provisoire. Cemagref, Agence de l'Eau Rhône-Méditerranée-Corse, Onema, Lyon (45 pp.).

Le Moal, Morgane, Chantal Gascuel-Odoux, Alain Ménesguen, Yves Souchon, Claire Étrillard, Alix Levain, Florentina Moatar et al. (2019). Eutrophication: a new wine in an old bottle?. Science of the Total Environment, 651, 1-11. doi: https://doi.org/10.1016/j.scitotenv.2018.09.139.

Lehner, B., Liermann, C. R., Revenga, C., Vörösmarty, C., Fekete, B., Crouzet, P., ... & Nilsson, C. (2011). High-resolution mapping of the world's reservoirs and dams for sustainable river-flow management. Frontiers in Ecology and the Environment, 9(9), 494-502. doi: 10.1890/100125.

Lessard, J. L., & Hayes, D. B. (2003). Effects of elevated water temperature on fish and macroinvertebrate communities below small dams. River research and applications, 19(7), 721-732. doi:https://doi.org/10.1002/rra.713.

Lowney, C. L. (2000). Stream temperature variation in regulated rivers: Evidence for

754 a spatial pattern in daily minimum and maximum magnitudes. Water Resources
755 Research, 36(10), 2947-2955. doi: https://doi.org/10.1029/ 2000WR900142.
756 Maheu, A., St-Hilaire, A., Caissie, D., El-Jabi, N., Bourque, G., & Boisclair, D. (2016a).
757 A regional analysis of the impact of dams on water temperature in medium-size
758 rivers in eastern canada. *Canadian Journal of Fisheries and Aquatic Sciences*, *73* ,
759 1885–1897. doi: https://doi.org/10.1139/cjfas-2015-0486.
760 Maheu, A., St-Hilaire, A., Caissie, D., & El-Jabi, N. (2016b). Understanding the thermal
761 regime of rivers influenced by small and medium size dams in Eastern Canada.
762 River Research and Applications, 32(10), 2032-2044. doi:
763 https://doi.org/10.1002/rra.3046.
764 Maxted, J. R., McCready, C. H., & Scarsbrook, M. R. (2005). Effects of small ponds
765 on stream water quality and macroinvertebrate communities. New Zealand
766 Journal of Marine and Freshwater Research, 39(5), 1069-1084. doi:
767 https://doi.org/10.1080/00288330.2005.9517376.
768 Mayer, T. D. (2012). Controls of summer stream temperature in the Pacific Northwest.
769 Journal of Hydrology, 475, 323-335. doi:
770 https://doi.org/10.1016/j.jhydrol.2012.10.012.
771 McMillan, H., Westerberg, I., & Branger, F. (2017). Five guidelines for selecting
772 hydrological signatures. doi: https://doi.org/10.1002/hyp.11300.
773 Michel, A., Brauchli, T., Lehning, M., Schaefli, B., & Huwald, H. (2020). Stream
774 temperature and discharge evolution in Switzerland over the last 50 years:
775 annual and seasonal behaviour. Hydrology and earth system sciences, 24(1),
776 115-142.doi: https://doi.org/10.5194/hess-24-115-2020.
777 Minaudo, C., Curie, F., Jullian, Y., Gassama, N., & Moatar, F. (2018). QUAL-NET, a
778 high temporal-resolution eutrophication model for large hydrographic networks.
779 Biogeosciences, 15(7). doi: https://doi.org/10.5194/bg-15-2251-2018.
780 Moatar, F., & Gailhard, J. (2006). Water temperature behaviour in the River Loire since
781 1976 and 1881. Comptes Rendus Geoscience, 338(5), 319-328. doi:

https://doi.org/10.1016/j.crte.2006.02.011.

Mohseni, O., Erickson, T. R., & Stefan, H. G. (1999). Sensitivity of stream temperatures in the United States to air temperatures projected under a global warming scenario. Water Resources Research, 35(12), 3723-3733. doi: 10.1029/1999WR900193.

Niemeyer, R. J., Cheng, Y., Mao, Y., Yearsley, J. R., & Nijssen, B. (2018). A thermally stratified reservoir module for large-scale distributed stream temperature models with application in the Tennessee River Basin. Water Resources Research, 54(10), 8103-8119. doi: https://doi.org/10.1029/2018WR022615.

O'Driscoll, M. A., & DeWalle, D. R. (2006). Stream–air temperature relations to classify stream–ground water interactions in a karst setting, central Pennsylvania, USA. Journal of Hydrology, 329(1-2), 140-153. doi: https://doi. org/10.1016/j.jhydrol.2006.02.010.

Olden, J. D., & Naiman, R. J. (2010). Incorporating thermal regimes into environmental flows assessments: modifying dam operations to restore freshwater ecosystem integrity. Freshwater Biology, 55(1), 86-107. doi: https://doi.org/10.1111/j.1365-2427.2009.02179.x.

Pella, H., Lejot, J., Lamouroux, N., & Snelder, T. (2012). Le réseau hydrographique théorique (RHT) français et ses attributs environnementaux. Géomorphologie: relief, processus, environnement, 18(3), 317-336. doi: https://doi.org/10.4000/geomorphologie.9933.

Petts, G. E., & Gurnell, A. M. (2005). Dams and geomorphology: research progress and future directions. Geomorphology, 71(1-2), 27-47. doi: https://doi.org/10.1016/j.geomorph.2004.02.015.

Pilgrim, J. M., Fang, X., & Stefan, H. G. (1998). STREAM TEMPERATURE CORRELATIONS WITH AIR TEMPERATURES IN MINNESOTA: IMPLICATIONS FOR CLIMATE WARMING 1. JAWRA Journal of the American Water Resources Association, 34(5), 1109-1121 doi: https://doi.org/10.1111/j.1752-1688.1998.tb04158.x..

Poole, G. C., & Berman, C. H. (2001). Profile: an ecological perspective on in-stream temperature: natural heat dynamics and mechanisms of human-cause thermal degradation. Journal of Environmental Management, 27, 787-802. doi: https: //doi.org/10.1007/s002670010188.

Preece, R. M., & Jones, H. A. (2002). The effect of Keepit Dam on the temperature regime of the Namoi River, Australia. River Research and Applications, 18(4), 397-414. doi: https://doi.org/10.1002/rra.686.

Quintana-Segui, P., Le Moigne, P., Durand, Y., Martin, E., Habets, F., Baillon, M., ... & Morel, S. (2008). Analysis of near-surface atmospheric variables: Validation of the SAFRAN analysis over France. Journal of applied meteorology and climatology, 47(1), 92-107. doi: https://doi.org/10.1175/2007JAMC1636.1.

Team, R. C. (2013). R: A language and environment for statistical computing. URL: http://www.R-project.org/.

Sauquet, E., & Catalogne, C. (2011). Comparison of catchment grouping methods for flow duration curve estimation at ungauged sites in France. doi: 10.5194/hess-15-2421-2011.

Sauquet, E., Gottschalk, L., & Leblois, E. (2000). Mapping average annual runoff: a hierarchical approach applying a stochastic interpolation scheme. Hydrological sciences journal, 45(6), 799-815. doi: https://doi.org/10.1080/02626660009492385.

Schmadel, N. M., Harvey, J. W., Alexander, R. B., Schwarz, G. E., Moore, R. B., Eng, K., ... & Scott, D. (2018). Thresholds of lake and reservoir connectivity in river networks control nitrogen removal. Nature communications, 9(1), 1-10. doi: https://doi.org/10.1038/s41467-018-05156-x.

Sinokrot, B. A., Stefan, H. G., McCormick, J. H., & Eaton, J. G. (1995). Modeling of climate change effects on stream temperatures and fish habitats below dams and near groundwater inputs. Climatic Change, 30(2), 181-200.doi: https://doi.org/10.1007/BF01091841.

Smith, K., & Lavis, M. E. (1975). Environmental influences on the temperature of a

small upland stream. Oikos, 228-236. doi: https://doi.org/10.2307/3543713.

Steel, E. A., Beechie, T. J., Torgersen, C. E., & Fullerton, A. H. (2017). Envisioning, quantifying, and managing thermal regimes on river networks. BioScience, 67(6), 506-522. doi: https://doi.org/10.1093/biosci/bix047.

Steel, E. A., & Lange, I. A. (2007). Using wavelet analysis to detect changes in water temperature regimes at multiple scales: Effects of multi-purpose dams in the Willamette River basin. River Research and Applications, 23(4), 351-359. doi: https://doi.org/10.1002/rra.985.

Stefan, H. G., & Preud'homme, E. B. (1993). Stream temperature estimation from air temperature 1. JAWRA Journal of the American Water Resources Association, 29(1), 27-45. doi: https://doi.org/10.1111/j.1752-1688. 1993.tb01502.x.

Valette, L., Piffady, J., Chandesris, A., & Souchon, Y. (2012). SYRAH-CE: description des données et modélisation du risque d'altération hydromorphologique des cours d'eau pour l'état des lieux DCE. Rapport Technique Onema-Irstea. URL: http://oai.afbiodiversite.fr/cindocoai/download/PUBLI/1185/1/2012_108.pdf_4080 Ko.

Van Vliet, M. T. H., Yearsley, J. R., Franssen, W. H. P., Ludwig, F., Haddeland, I., Lettenmaier, D. P., & Kabat, P. (2012). Coupled daily streamflow and water temperature modelling in large river basins. Hydrology and Earth System Sciences, 16(11), 4303-4321. doi: 10.5194/hess-16-4303-2012.

Venables, W. N., & Ripley, B. D. (2002). Modern Applied Statistics with S 4th ed New York Springer. URL: http://www.stats.ox.ac.uk/pub/MASS4.

Verneaux, J. (1977). BIOTYPOLOGIE DE L'ECOSYSTEME" EAU COURANTE". DETERMINISME APPROCHE DE LA STRUCTURE BIOTYPOLOGIQUE.

Vidal, J. P., Martin, E., Franchistéguy, L., Baillon, M., & Soubeyroux, J. M. (2010). A 50-year high-resolution atmospheric reanalysis over France with the Safran system. International Journal of Climatology, 30(11), 1627-1644. doi: https://doi.org/10.1002/joc.2003.

866 Vörösmarty, C. J., Meybeck, M., Fekete, B., Sharma, K., Green, P., & Syvitski, J. P.
867 (2003). Anthropogenic sediment retention: major global impact from registered
868 river impoundments. Global and planetary change, 39(1-2), 169-190. doi:
869 https://doi.org/10.1016/S0921-8181(03)00023-7.
870 Yearsley, J. R., Sun, N., Baptiste, M., & Nijssen, B. (2019). Assessing the impacts of
871 hydrologic and land use alterations on water temperature in the Farmington River
872 basin in Connecticut. Hydrology and Earth System Sciences, 23(11), 4491-4508.
873 doi: https://doi.org/10.5194/hess-23-4491-2019.
874 Webb, B. W. (1996). Trends in stream and river temperature. Hydrological processes,
875 10(2), 205-226. doi: https://doi. org/10.1002/(SICI)1099-
876 1085(199602)10:2<205::AID-HYP358>3.0.CO;2-1.
877 Webb, B. W., & Walling, D. E. (1993). Temporal variability in the impact of river
878 regulation on thermal regime and some biological implications. Freshwater
879 Biology, 29(1), 167-182. doi: https://doi.org/10.1111/j.1365-2427. 1993.tb00752.x.
880 Webb, B. W., & Walling, D. E. (1996). Long-term variability in the thermal impact of
881 river impoundment and regulation. Applied Geography, 16(3), 211-223. doi:
882 https://doi.org/10.1016/0143-6228(96)00007-0.
883 Webb, B. W., & Walling, D. E. (1997). Complex summer water temperature behaviour
884 below a UK regulating reservoir. Regulated Rivers: Research & Management: An
885 International Journal Devoted to River Research and Management, 13(5), 463-477.
886 doi: https://doi.org/10.1002/(SICI)1099-1646(199709/10)13:5<463::AID-
887 RRR470>3.0.CO;2-1.
888 Webb, B. W., & Zhang, Y. (1997). Spatial and seasonal variability in the components of
889 the river heat budget. Hydrological processes, 11(1), 79-101. doi:
890 https://doi.org/10.1002/(SICI)1099-1085(199701)11:1<79:: AID-
891 HYP404>3.0.CO;2-N.
892 Webb, B. W., Hannah, D. M., Moore, R. D., Brown, L. E., & Nobilis, F. (2008). Recent
893 advances in stream and river temperature research. Hydrological Processes: An

894 International Journal, 22(7), 902-918. doi: https: //doi.org/10.1002/hyp.6994

List of Figures

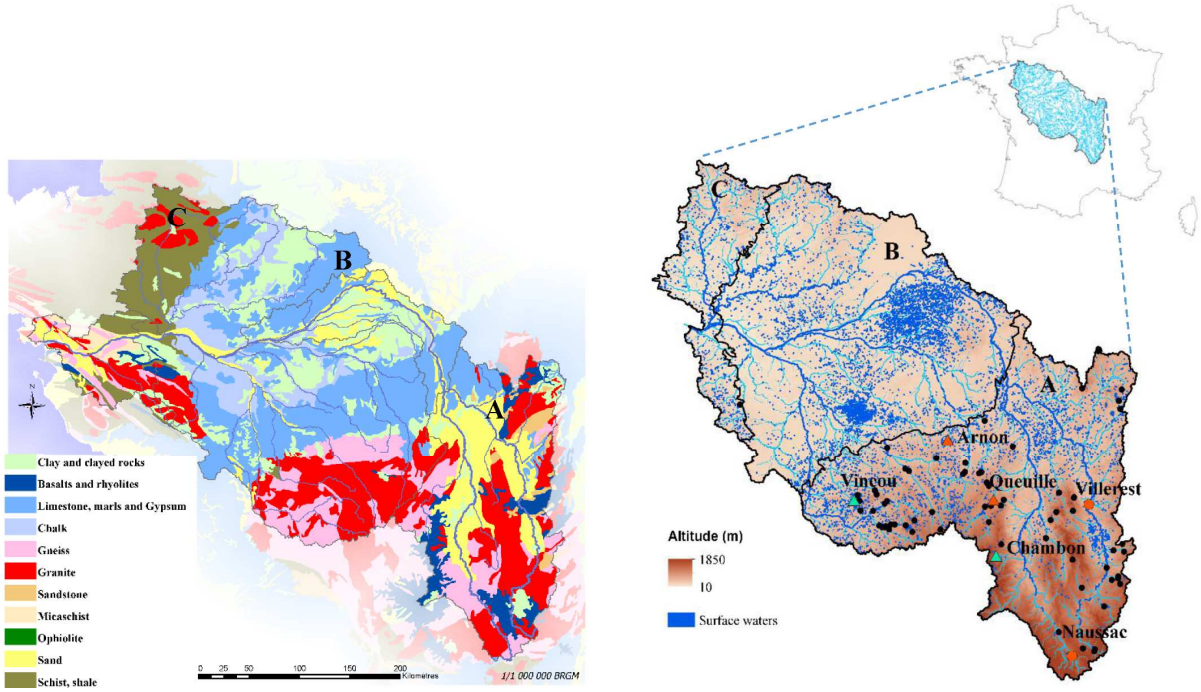

Figure 1: The Loire River basin. Left panel: main aquifer formations and basin lithology; granite and basalt dominate the upstream part of the basin (Region A), whereas sedimentary rocks occupy the middle reaches with a potential for ground water input (Region B), which leads to more granite and schist in the lower reaches (Region C). Right panel: altitude and surface waters. Black points show dams higher than 15 m. Red circle points show the two largest dams in the basin. Triangles denote stations that had a potential for upstream-downstream comparison (red for dams, green for ponds), which are visually assessed in Supplementary Figure 2.

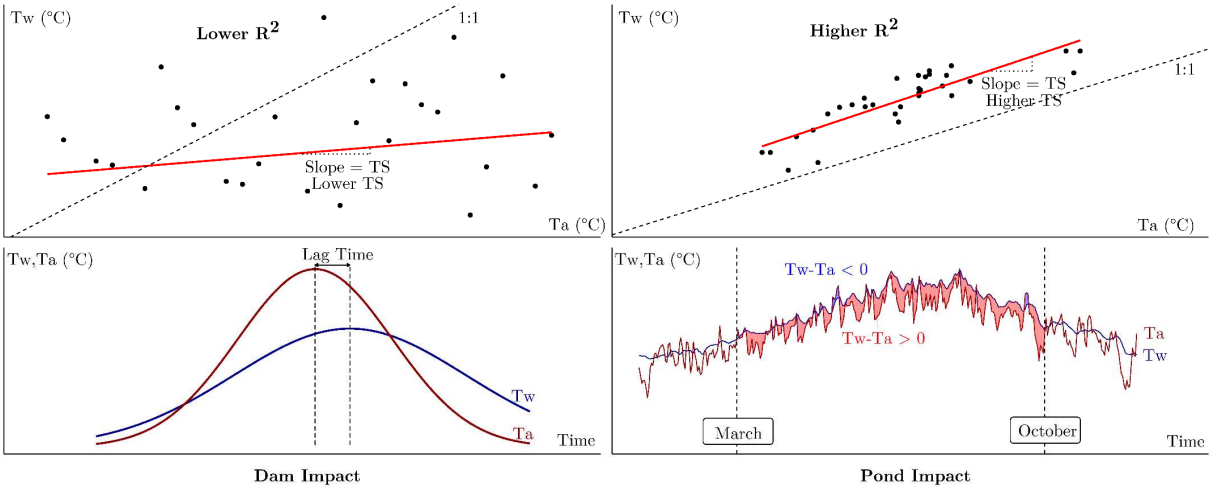

Figure 2: Conceptual representation of thermal signatures. Top row: daily stream-air temperature linear regression showing lower TS (Thermal Sensitivity) and lower R^2 downstream of a dam (left), and higher TS and higher R^2 downstream of ponds (right). Bottom row: stream and air temperature regimes showing the lagged annual cycle of stream temperature relative to air temperature downstream of a dam (left), and greater heating effect and thermal effect more often downstream of ponds (right). See Table 1 for the mathematical definition of thermal signatures.

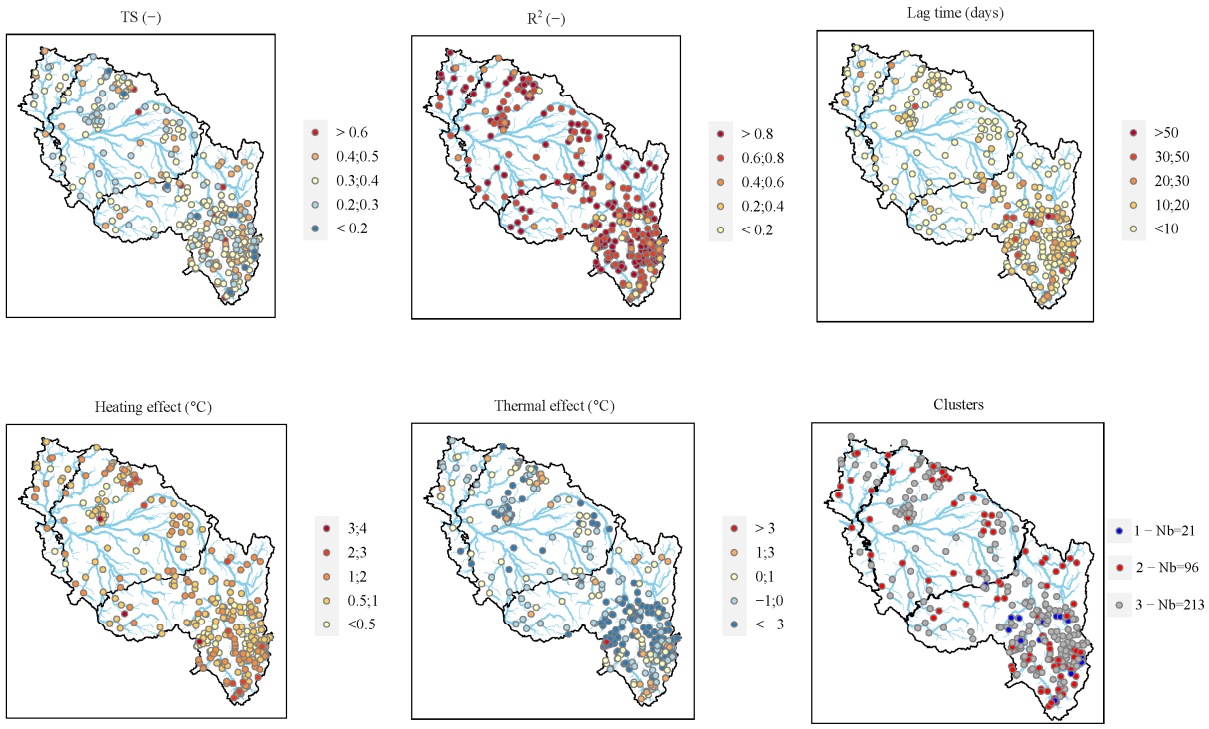

Figure 3: Spatial distribution of the five thermal indicator values over 330 stations on the Loire basin, and spatial distribution of the stations in three obtained clusters, or thermal signatures (bottom right). The top row were expected dam thermal indicators and the bottom row (i.e., heating and thermal effects) were expected pond thermal indicators.

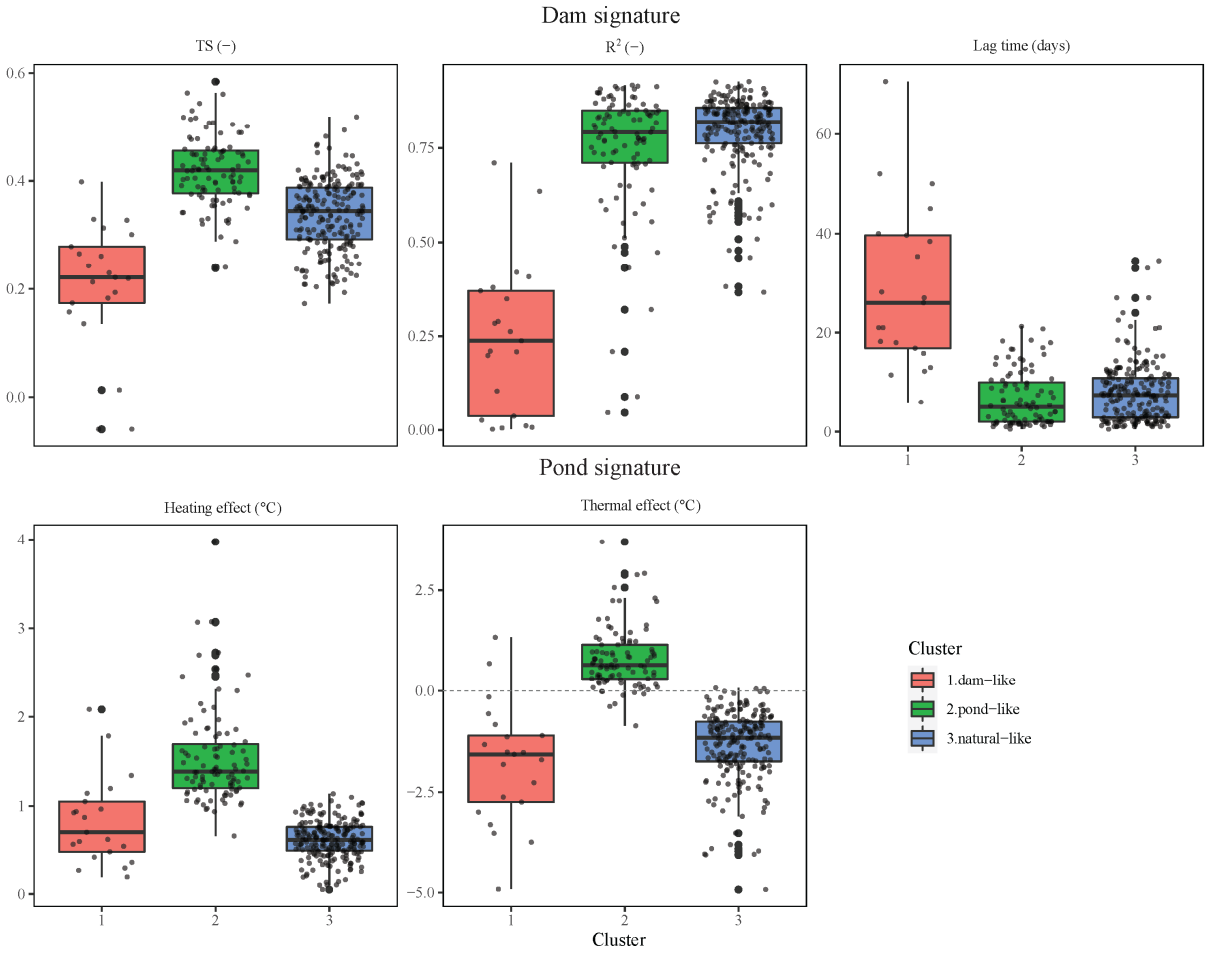

Figure 4: Statistical distribution of thermal signatures in each cluster: 1.dam-like with 21 stations; 2.pond-like with 96 stations; 3.natural-like with 213 stations.

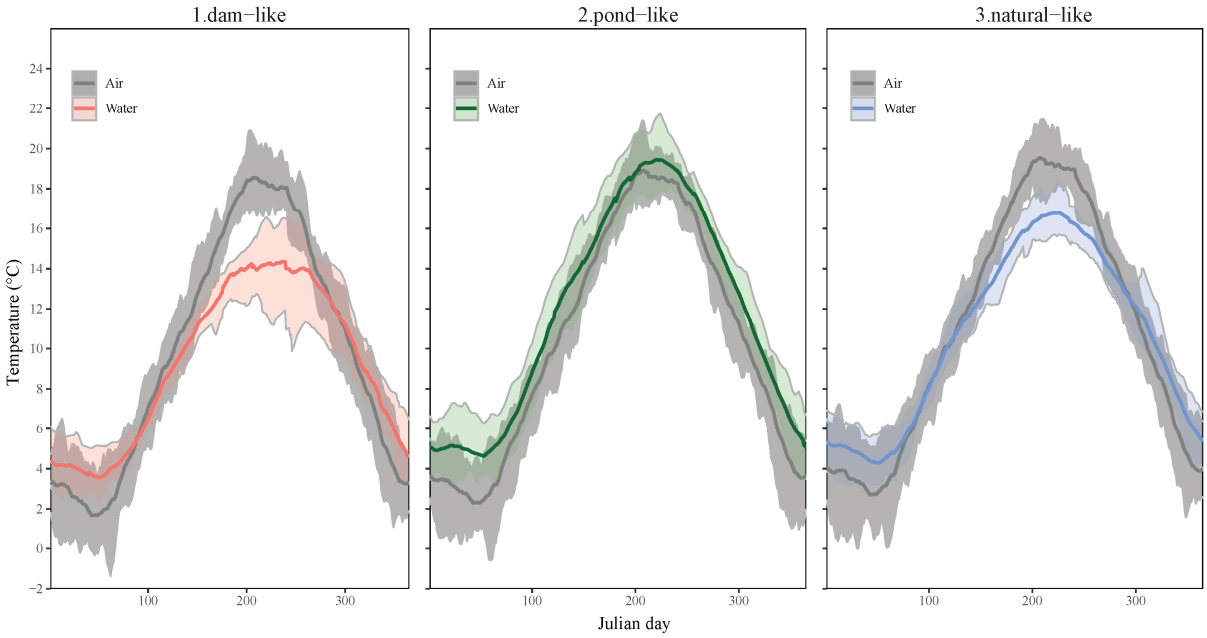

Figure 5: The annual air and water temperature regimes of altered (by dams and ponds) and natural streams. Shaded areas represent the 10th-90th percentile band, and solid lines represent the median value: 1.dam-like with 15 stations that have a large upstream dam; 2.pond-like with 90 stations; 3.natural-like with 213 stations.

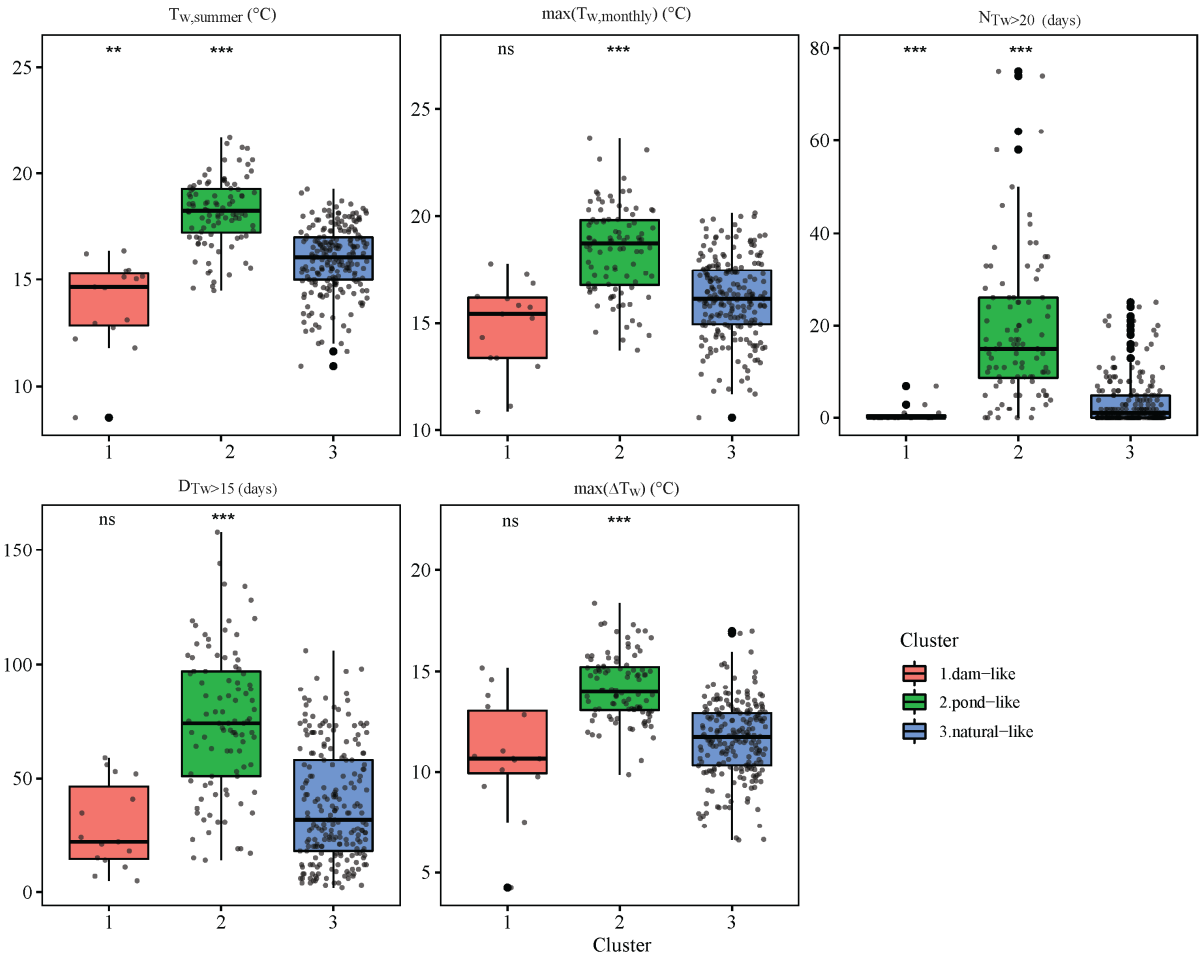

Figure 6: Statistical distribution of ecologically relevant thermal metrics in each cluster: 1) dam-like with 15 stations that have a large upstream dam, 2) pond-like with 90 stations, and 3) natural-like with 213 stations. The t-test was conducted with the reference group of natural-like cluster. ***, **, and * indicates that the metric for the group of altered regimes is significantly different from natural regimes at the 1, 5 and 10% confidence levels, respectively. The “ns” shows that the metric for the group of altered regime is non-significantly different from natural regimes.

List of Tables

Table 1: Indicators used to identify thermal signatures of altered stream temperature regimes. Indicators are grouped into a dam or pond signature based on their hypothesized ability to detect thermal effects from their respective anthropogenic structures.

Indicator	Definition	Rationale
	Dam signature	
Thermal sensitivity (TS)	Daily JJA stream-air temperature linear regression slope	Dams reduce TS
R^2	Daily JJA stream-air temperature coefficient of determination	Dams reduce R^2
Lag time	Lag time between the annual peak in 30-days moving average stream and air temperature regimes	Dams increase lag time
	Pond signature	
Heating effect	mean positive difference of daily stream-air temperature difference (T_w-T_a) from March–October	Ponds increase distributed energy storage, leading to heating
Thermal effect	mean overall difference of daily stream-air temperature difference (T_w-T_a) from March–October	Ponds increase energy storage, even in the presence of natural cooling

Note: Indicators are calculated based on interannual averages

Table 2: Descriptive variables tested for assessing the links between thermal signatures and dam/pond characteristics (see Section 3.4). Mean and standard deviation values (SD) are shown for the 330 stations selected in the study (see Section 3.1).

Notation	Variable	Mean	SD	Unit
	dam/pond characteristics			
d_{dam}	Distance from the closest large dam [a]	6.6	4.2	km
IRI	Impounded Runoff Index of the closest large dam [b]	11	16	%
IRI/d_{dam}	IRI/distance from the closest large dam [c]	10	25.5	%/km
$f_{pond,reach}$	Fraction of station's reach surface area that is ponded [d]	7.5	12	%
$\overline{f}_{pond,reach}$	Fraction of station's reach surface area that is ponded; averaged over all upstream reaches	1.6	2.7	%
$f_{pond,catchment}$	Fraction of the catchment area that is ponded [e]	0.17	0.8	%
	catchment properties			
T_a	Annual mean T_a at station	12	1.5	°C
$A_{catchment}$	Catchment area	232	300	km^2
Alt	Altitude at station	399	290	m
S	Upstream mean slope	0.037	0.03	m/km
D	Distance from the source	30	20	km
W_q	Width for median discharge [f]	8.7	6.3	m
D_q	Depth for median discharge [f]	0.3	0.16	m
q	Mean annual specific discharge [g]	10	4.9	$l/s/km^2$
CI	Connectivity index [h]	0.4	0.08	-
Veg	Rate of vegetation cover [i]	83	22	%

[a] Derived from ArcMap tools.
[b] Ratio of dam volume to mean annual runoff.
[c] To capture the interaction between the dam characteristic and the position of a station from the dam.
[d] Extracted from SYRAH-CE database (Valette et al., 2012). Final nodes of each considered river segment are at important confluences and topologically important places.
[e] A proxy of cumulative effects of upstream ponds.
[f] From the ESTIMKART empirical model developed by Lamouroux et al. (2010).
[g] Based on geostatistical interpolation on the RHT network (Pella et al., 2012; Sauquet et al., 2000).
[h] IC: Q10-Q99/Q1-Q99; represents the shape of the dimensionless flow duration curve. This descriptor is a measure of the contrast between low-flow and high-flow regimes. Values close to 1 are observed where there are large aquifers or storage in snow packs. Values close to 0 are related to catchments exposed to contrasted weather (Sauquet & Catalogne, 2011).
[i] Derived from remote sensing on both sides of reaches with a buffer of 10 m at station, as reported in SYRAH-CE database (Valette et al., 2012).

Table 3: Selected ecologically relevant thermal metrics for comparison between altered regimes and natural ones.

Regime feature	Metric	Description	Biological importance
Magnitude	$\overline{T}_{w,summer}$	Mean T_w in summer (June–August)	Differences in mean temperature across river systems contribute to determining which species are present and which are absent
	$\max(T_{w,monthly})$	Maximum of the 30-day moving average daily mean T_w	Used in the biotypology according to the formula proposed by Verneaux et al. (1977)
Frequency	$N_{Tw>20}$	Number of days that daily mean T_w>20 °C	Species-specific differences in response to high temperatures provide preferential advantages to particular species
Duration	$D_{Tw>15}$	Duration of consecutive days with mean T_w>15°C	Accumulated stress may trigger migration and other major life-history transitions
Rate of change	$\max(\Delta T_w)$	Difference between mean T_w in August and February	The competitive advantage of one species over another may be determined by conditions in both summer and winter [a]

[a] Buisson & Grenouillet (2009) used air temperature instead of water temperature.

Table 4: Stepwise multiple linear regression results for cross-validation approach relating descriptive variables for thermal indicators within dam and pond signatures. ***, **, and * denote significance at the 1, 5 and 10% confidence levels, respectively. The scaled coefficients are shown in parentheses for comparison among predictor variables.

	Dam signature		
Descriptive variable	**TS (-)**	**R^2 (-)**	**Lag time (days)**
S [m/km]	—	—	232.85±92.891** (0.377±0.151)
d_{dam} [km]	0.015±0.005*** (0.458±0.140)	0.029±0.010** (0.385±0.141)	-1.6±0.560*** (-0.425±0.151)
IRI [%]	-0.002±0.001** (-0.306±0.145)	-0.009±0.002*** (-0.484±0.146)	—
Adjusted R^2	0.43	0.482	0.3
F statistic (df)	12.37 (29)	15.43 (29)	7.64 (29)
p-value	<0.001	<0.001	0.002
	Pond signature		
Descriptive variable	**Heating effect (°C)**	**Thermal effect (°C)**	
Veg [%]	-0.003±0.002* (-0.164±0.102)	—	
$f_{pond,catchment}$ [%]	0.62±0.211*** (0.296±0.102)	0.762±0.305** (0.257±0.102)	
Adjusted model R^2	0.1	0.060	
F statistic (df)	5.442 (87)	3.872 (87)	
p-value	0.006	0.024	

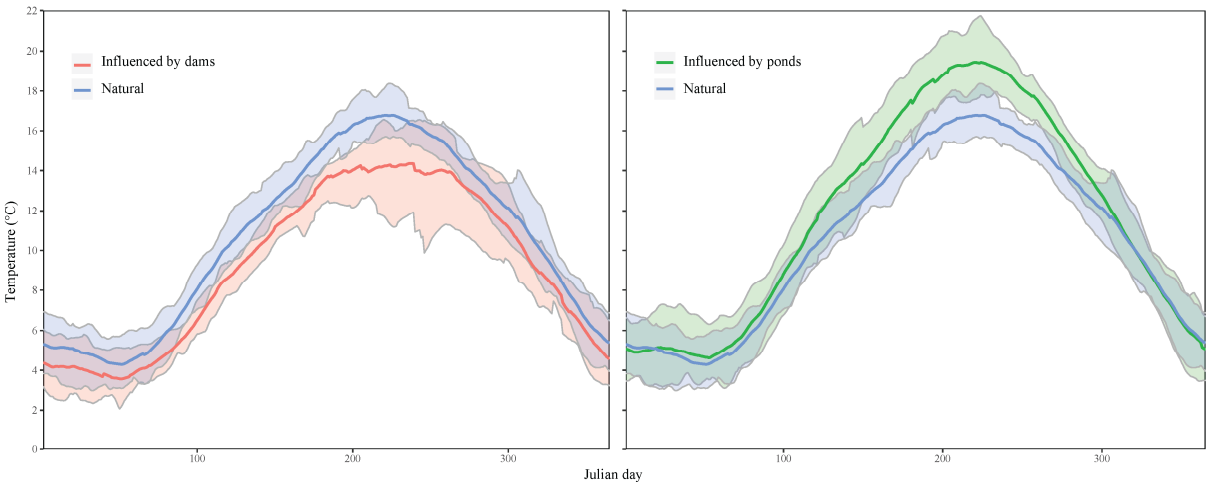
Influenced by dams
Natural
Influenced by ponds
Natural
Temperature (°C)
Julian day
0
2
4
6
8
10
12
14
16
18
20
22
100
200
300